Industrial Engineering Journal
ISSN: 0970-2555
Volume : 54, Issue 8, No.1, August : 2025

SOLAR DRYER SIMULATION AND ENERGY ANALYSIS USING CFD: A REVIEW AND CASE STUDY

Mr. Salik Ram Dhimar, Research Scholar, Shri Rawatpura Sarkar University, Raipur Chhattisgarh
Dr. Ajay Kumar Gupta Associate Professor, Department of mechanical Engineering, Shri Rawatpura Sarkar University, Raipur, Chhattisgarh India
Dr. Pankaj Kumar*, Assistant Professor, GMR Institute of Technology, Rajam, A.P.-532127
Mr. Sunil Sharma Assistant Professor, Department of Mechanical Engineering, Shri Rawatpura Sarkar University, Raipur, Chhattisgarh India
Mr. Anand Kumar Sahu, Research Scholar, Shri Rawatpura Sarkar University, Raipur Chhattisgarh India
Mr. Suresh Chandra Dansena, Research Scholar, Shri Rawatpura Sarkar University, Raipur Chhattisgarh India

ABSTRACT

Solar food drying is a well-established technique for food preservation in India. Over the years, numerous solar dryer models have been developed and validated through experimental trials and numerical simulations, both of which are typically time- and cost-intensive. Computational Fluid Dynamics (CFD) offers an efficient alternative by enabling accurate model simulations in a shorter time frame. This study focuses on CFD-based simulation, validation, energy analysis, and numerical modelling of a domestic direct-type multi-shelf solar dryer. Experimental investigations were carried out in Chhattishgarh during November 2006.

The simulation process includes:

- Detailed structural and material specifications of each system component,
- Application of conservation equations across the mesh at defined time intervals, and
- Graphical representation of simulation results.

Mathioulakis et al. [6] simulated an industrial batch-type air dryer developed by Vencon-Varsos SA for fruit drying. Using CFD, they modelled airflow within the chamber and observed variations in drying levels across different trays, indicating non-uniform drying. Their results established a strong correlation between air velocity and drying rate, affirming CFD's effectiveness as a design optimization tool that can reduce the need for costly experimental trials.

Romero et al. [5] employed ANSYS Fluent to simulate and validate the vanilla drying process in an indirect solar dryer. They found close alignment between simulation and experimental data at the air outlet, though some discrepancies were noted in the internal temperature distribution.

Papade and Boda [7] analyzed a 2D convergent-divergent section of an indirect solar dryer using CFD, while exploring the integration of phase change materials (PCMs) to enhance efficiency and enable nighttime operation.

Sonthawi et al. [8] designed a solar biomass hybrid dryer for natural rubber sheets and validated their simulation using ANSYS Fluent. Their study showed close agreement between simulated and experimental values. The simulation helped visualize air flow distribution and confirmed that the moisture content in rubber sheets was reduced from 34.26% to 0.34% in 48 hours.

This study emphasizes the simulation of a domestic direct-type multi-shelf solar dryer under no-load conditions using ANSYS Fluent 14.0. The aim is to guide researchers on CFD applications and design validation in solar drying systems, reducing the cost associated with trial-and-error physical testing. The energy analysis performed confirms the system's effectiveness and environmental benefits. Notably, there has been limited work on the CFD simulation of compact, domestic multi-shelf dryers—highlighting the significance of this study.

Key simulation outcomes include:

- Air temperature inside the dryer reached 326 K, confirming the design's efficiency.

- Embodied energy of the dryer components was calculated at 339.015 kWh.
- The energy payback time was estimated at 7.57 years, with a carbon credit of INR 2055.
- The convective heat transfer coefficient ranged from 2.4 to 2.8 W/m²°C.
- The coefficient of determination (R^2) was found to be 0.98, indicating strong agreement between simulated and experimental results.

Keywords: Solar dryer · CFD simulation · Numerical modeling · Embodied energy · ANSYS Fluent

I. Introduction

In countries like India, the concept of food drying dates back centuries. Traditionally, open sun drying was used for fruits, vegetables, spices, and other crops. However, this method has multiple limitations: exposure to adverse weather, contamination by insects and animals, and inconsistent drying quality. To overcome these issues, solar drying under controlled conditions was introduced.

Solar dryers are economical, environmentally friendly, and especially beneficial for domestic users. Typically constructed using affordable, locally available materials like wood, aluminum sheets, and wire mesh, these dryers have a short payback period and zero operating cost due to their reliance on freely available solar energy.

Solar dryers are generally categorized based on the mode of solar radiation usage:

- **Direct-type:** Solar radiation directly dries the food placed inside a cabinet or greenhouse-type chamber.
- **Indirect-type:** Air is heated separately and then circulated inside the drying chamber, offering better product quality.
- **Mixed-mode:** Combines features of both direct and indirect systems, offering faster and more efficient drying.

Based on the airflow mechanism, dryers can also be classified as:

- **Passive (natural convection)**
- **Active (forced convection)**

Figure 1 illustrates these classifications [2].

II. Role of CFD in Solar Dryer Design

CFD (Computational Fluid Dynamics) is a field of fluid mechanics that applies numerical analysis and algorithms to study fluid flow. Using mathematical modeling and powerful computing tools, CFD can simulate the interaction of fluids with defined boundary conditions, reducing the need for repeated physical prototyping.

ANSYS Fluent is one such advanced CFD software used extensively in industrial and academic research. It allows for simulation of mass, momentum, and heat transfer, making it ideal for optimizing solar dryer designs. CFD simulations provide precise results for air flow, temperature profiles, and drying rates—empowering researchers to validate and improve designs with minimal resource expenditure.

III. Simulation Methodology

To perform CFD simulations using ANSYS Fluent, the following steps are typically followed [5]:

- **Geometry design and meshing** using CAD software or ANSYS Design Modeler.
- **Specification of material properties and boundary conditions** for each system component.
- **Application of conservation equations** (mass, momentum, and energy) over the control volume.
- **Numerical simulation** under defined initial and boundary conditions.
- **Post-processing** for visualization and interpretation of temperature, velocity, and energy data.

List of Symbols and Notations

Symbol	Description
a	Absorptivity or absorption coefficient
s, s'	Direction vector of sun, Scattering direction vector
r	Position vector
I	Radiation intensity
T	Local temperature
n	Refractive index
σ	Stefan–Boltzmann constant
TS, Ta	Stagnation temperature, Ambient temperature
Ed, gd	Daily thermal output, Daily system efficiency
K	Latent heat of vaporization
Ean, Ein	Annual thermal output, Daily input energy
h_{cvt}	Convective heat transfer coefficient
X	Peak temperature inside dryer
Ig	Global solar radiation intensity
M	Mass of evaporated moisture
Dc	Carbon credit value
Q_{hlf}	Heat loss factor
DP	Partial pressure of air
P(T)	Saturated vapor pressure
Ah, At	Area of holes, Heat wall area

IV. Design And Description Of Dryer

A domestic direct-type multi-shelf solar dryer (Fig. 2), designed by Singh et al. [9], was tailored for Indian conditions, particularly for use in Chhattishgarh (31°N latitude). The dryer comprises three perforated trays arranged vertically to facilitate natural air circulation. Its inclination is adjustable to maximize solar radiation capture, and it was aligned according to Chhattishgarh's latitude for optimal performance.

Key structural components include a base frame, drying trays, a box enclosure, and shading plates. The frame was fabricated using 19 mm × 19 mm × 1.6 mm thick iron angles. Thermal insulation of 5 cm thick thermocol was applied to the top, back, one side wall, and door. To ensure air exchange, 40 holes of 8 mm diameter were provided at the bottom and 20 at the top. A 4 mm thick glass sheet was mounted on the front side for glazing, and the internal surfaces were painted black to improve solar absorption.

Each drying tray had an area of 0.105 m² and was supported by metal brackets. The inclination was fixed at 45° during experimental observations conducted under no-load conditions in November.

V. Experimental Setup Details:

- The dryer was tested in Chhattishgarh (31°N) under no-load conditions.
- All exhaust vents were sealed to achieve maximum stagnation temperature.
- Orientation: South-facing, operational from 9:30 AM to 4:00 PM.

Industrial Engineering Journal
ISSN: 0970-2555
Volume : 54, Issue 8, No.1, August : 2025

Figure 2 Direct type Domestic multi shelf dryer front and isometric view

Grid Nodes	Thermal Efficiency (%)
206,412	36.5
210,853	36.7
288,463	**37.0**

The average overall heat loss coefficient U_I was estimated using the relation:

$$I(\tau\alpha)=U_1(T_s-T_a)$$

Where:

- I: Solar radiation intensity (W/m²)
- τ: Transmissivity
- α: Absorptivity
- T_s: Maximum stagnation temperature
- T_a: Ambient temperature

Key Observations:

- Maximum stagnation temperature: 100 °C
- Ambient temperature: 30 °C
- Solar radiation intensity: 750 W/m² at noon
- Heat loss coefficient U1U_1U1: 8.5 W/m²·K, lower than comparable dryers

VI. CFD Simulation Approach

To simulate airflow and temperature distribution inside the dryer, ANSYS Fluent 14.0 was used. The model requires solving fundamental governing equations:

1. **Continuity (Mass Conservation)**:

$$\frac{\partial \rho}{\partial t} + \nabla \cdot (\rho \vec{v}) = 0$$

2. **Momentum Conservation**:

$$\frac{\partial (\rho \vec{v})}{\partial t} + \nabla \cdot (\rho \vec{v} \vec{v}) = -\nabla p + \rho \vec{g} + \vec{F}$$

Industrial Engineering Journal
ISSN: 0970-2555
Volume : 54, Issue 8, No.1, August : 2025

3. **Energy Conservation**:

$$\frac{\partial(\rho E)}{\partial t} + \nabla \cdot [\vec{v}(\rho E + p)] = 0$$

4. **Radiative Heat Transfer**:

$$\frac{dI(\vec{r},\vec{s})}{ds} + (\alpha + \sigma_s) I(\vec{r},\vec{s}) = \alpha n \int_{4\pi} I(\vec{r},\vec{s}')\Phi(\vec{s},\vec{s}')d\Omega',$$

The solar load model in ANSYS Fluent was activated to account for solar radiation using the solar calculator, set for Chhattishgarh (31°N, 75°E) on 21st November at noon.

Mesh Generation and Grid Independence Test:

- Air velocity: 5 m/s at inlet and outlet (8 mm diameter holes)
- Tray mesh size: 2 cm × 2 cm
- Nodes tested: 206,412 to 210,853
- Optimal mesh: 288,463 nodes (Fig. 6)
- Achieved thermal efficiency: ~37%

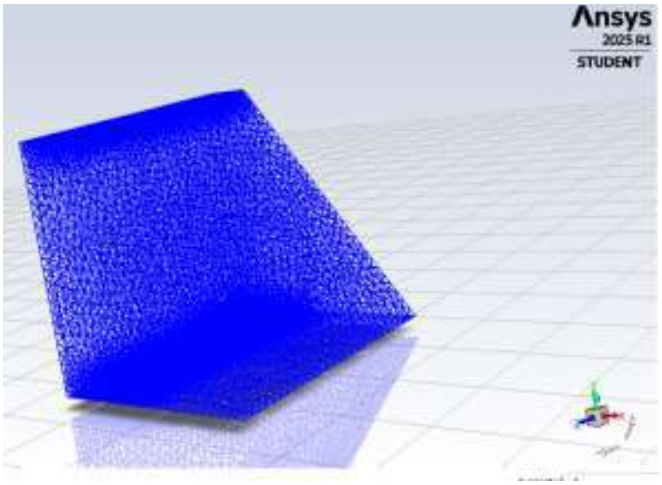

Figure 3.1 Wireframe View of the designed solar dryer

VII. Energy Analysis Of The Solar Dryer

Embodied Energy

The total embodied energy (EE) required for the construction of the dryer was calculated based on the material coefficients (Table 2). The cumulative embodied energy was found to be **339.02 kWh**.

Energy Payback Time (EPBT)

$$\text{EPBT} = \frac{\text{Embodied Energy}}{\text{Annual Energy Output}} = \frac{339.02}{44.77} = 7.57 \text{ years}$$

Carbon Emissions and Credit

- **CO_2 Emissions/year** (based on coal energy): 0.98 kg CO_2/kWh ⇒ 16.62 kg/year
- **CO_2 Mitigation** for fenugreek drying (150 days): 1.6 tonnes over lifetime
- **Carbon Credit Earned**: ₹2055 (based on \$18.97/tonne CO_2, conversion at ₹67.73/USD)

Thermal Performance Metrics

- **Dryer temperature**: Reached up to 328 K (simulation), aligned with experimental peak
- **Convective Heat Transfer Coefficient**: 2.4–2.8 W/m²·°C
- **Heat Utilization Factor (HUF)**: 0.69

- **Coefficient of Performance (COP)**: 0.46
- **Coefficient of Determination (R^2)**: 0.98, indicating excellent simulation accuracy
- CFD simulation using ANSYS Fluent effectively validated the design of the domestic direct-type solar dryer.
- Maximum dryer temperature and other thermal parameters aligned well with experimental data.
- The dryer exhibits low energy payback time and moderate carbon emissions, affirming its000 eco-friendly and cost-effective nature.
- Results confirm the viability of the design proposed by Singh et al. [9] for domestic solar drying of crops such as fenugreek and chillies.

IX. Results and Discussion

1. Air Pressure and Temperature Distribution

The simulation results revealed that the **gauge pressure inside the dryer cabinet increases with rising air temperature**. As shown in **Figure 7**, heated air molecules move upward due to buoyancy, resulting in a **higher pressure near the outlet** (top of the dryer) compared to the inlet (bottom). This pressure gradient enhances natural convection, facilitating effective drying.

2. Radiation Heat Flux and Absorption

Figures 9 and 10 present the **radiation heat flux contours** inside the solar dryer. The dryer walls and trays were assumed to have an absorptivity of **0.9**, consistent with experimental settings. Most of the incident solar radiation is absorbed internally, raising the cabinet temperature significantly. The **absorbed visible solar flux** is particularly high on the trays (Figure 10), which promotes rapid heating of circulating air — a critical factor in efficient food drying.

3. Embodied Energy and Material Contribution

The distribution of **embodied energy** for construction materials is presented in **Table 2 and Figure 11**. The **GI sheet, aluminum angles, and paint** account for the highest energy contribution during fabrication. The total **embodied energy** of the system was calculated to be **339.02 kWh**.

Table 2 Presented in embodied energy for construction materials.

S.No.	Time	Temperature Difference
1.	**At 11:00 AM:**	**ΔT = 12°C**
2.	At 12:00 PM:	**ΔT = 16°C**
3.	At 1:00 PM:	**ΔT = 9.5°C**
4.	At 2:00 PM:	**ΔT = 9°C**

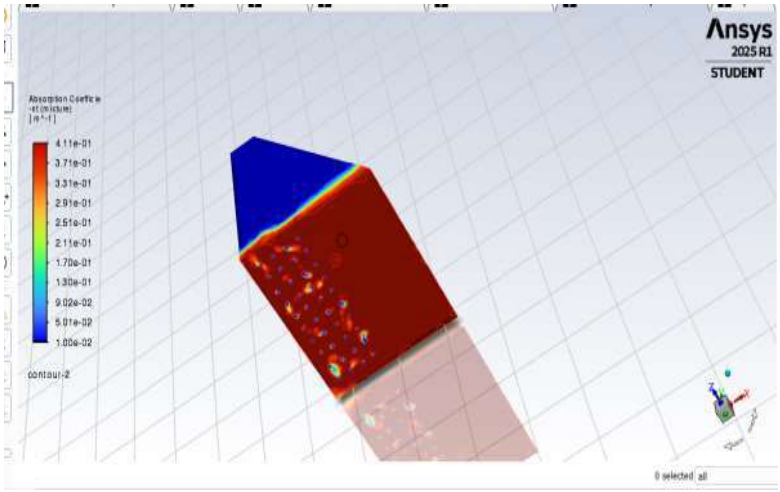

Figure 4.3 Static temperature distribution contour of absorber and glass

Industrial Engineering Journal
ISSN: 0970-2555
Volume : 54, Issue 8, No.1, August : 2025

4.2 Radiation Heat Flux and Absorption

Figures 9 and 10 present the **radiation heat flux contours** inside the solar dryer. The dryer walls and trays were assumed to have an absorptivity of **0.9**, consistent with experimental settings. Most of the incident solar radiation is absorbed internally, raising the cabinet temperature significantly. The **absorbed visible solar flux** is particularly high on the trays (Figure 10), which promotes rapid heating of circulating air a critical factor in efficient food drying.

Figure 4.4 Radiation heat flux distribution of dryer cabinet

4. Energy Payback Time (EPBT) and Environmental Impact

Due to the dryer's **simple construction** and **natural convection operation**, the **energy payback time (EPBT)** is relatively low at **7.57 years** (Table 3).

Annual CO_2 emissions are estimated to be **16.62 kg**, slightly higher than those from a cabinet-type dryer, attributed to this model's larger surface area and complexity (Figure 12). However, over a **20-year operational lifespan**, the system can mitigate up to **1.6 tonnes of CO_2**, assuming drying of **fenugreek leaves** for 150 days annually.

At a carbon credit rate of **$18.97/tonne CO_2** (as of 27/05/2018, 1 USD = ₹67.73), the **total carbon credit earned** is approximately **₹2055.26**.

5. Ambient Conditions and Thermal Performance

Ambient parameters significantly affect dryer performance. For Ludhiana (30.9010°N, 75.8573°E) in **November**, the ambient temperature ranged from **15°C to 23°C**, with an **average relative humidity of 76%**. **Global solar radiation** varied between **400 and 800 W/m²**, especially between **11:00 AM to 2:00 PM**.

These conditions contribute to a substantial temperature difference between the ambient and the dryer cabinet:

- At 11:00 AM: **ΔT = 12°C**
- At 12:00 PM: **ΔT = 16°C**
- At 1:00 PM: **ΔT = 9.5°C**
- At 2:00 PM: **ΔT = 9°C**

This temperature rise supports a **higher moisture removal rate**, crucial for drying vegetables and fruits.

6. Heat Transfer Characteristics

The **convective heat transfer coefficient (CHTC)** ranged from **2.4 to 2.8 W/m²·°C** during peak hours, indicating efficient thermal energy transfer from the absorber trays to circulating air.

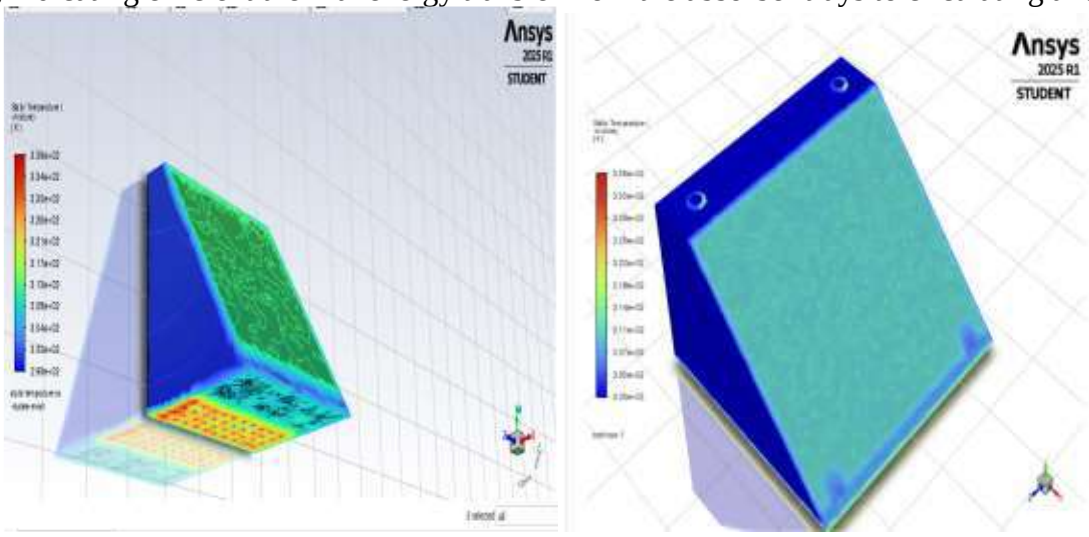

Figure 4.2 Static Temprature Distribution of dryer

Figure 8 shows static temperature contours inside the cabinet, with **peak air temperatures reaching up to 333 K** (~60°C), confirming effective heat retention.

7. Coefficient of Diffusivity and Heat Loss

The **coefficient of diffusivity** is influenced by solar radiation, ambient temperature, and internal air temperature. It was observed to be:

- **Low during morning**, due to insufficient heat buildup
- **Higher at noon**, signifying better air replacement and enhanced drying

Hourly heat loss values show a maximum loss of **3.15 W** at 2:00 PM, which remains **insignificant compared to the useful heat gain**.

The **Heat Utilization Factor (HUF)** and **Coefficient of Performance (COP)** were calculated as:

- **HUF**: 0.69
- **COP**: 0.46

These values reflect good thermal efficiency for a natural convection-based solar dryer.

8. Comparison Between Simulated and Experimental Results

Figure 13 compares **simulated dryer cabinet temperatures under natural convection** with **experimental stagnation temperatures** under no-load conditions. The peak temperatures obtained from simulation were **highly consistent with experimental data**, demonstrating the **reliability and validity** of the CFD model.

The **coefficient of determination (R^2)** for peak dryer temperatures was calculated as **0.98**, confirming an excellent correlation between the simulation and experimental results

References

1. Agarry, S.E., et al. (2005). Journal of Food Technology, 3(3), 361–364.
2. Jayaraman, K.S., & Gupta, D.K.D. (1992). Drying Technology, 10(1), 1–50.
3. Sevada, M.S., & Rathore, N.S. (2004). Journal of Agricultural Engineering, 41, 12–17.
4. Fudholi, A., et al. (2013). International Journal of Photoenergy, 2013, 1–9.